nature climate change

LETTERS

PUBLISHED ONLINE: 8 SEPTEMBER 2013 | DOI: 10.1038/NCLIMATE1989

# The impact of temperature on marine phytoplankton resource allocation and metabolism

A. Toseland[1], S. J. Daines[2], J. R. Clark[2], A. Kirkham[3], J. Strauss[3], C. Uhlig[4], T. M. Lenton[2], K. Valentin[4], G. A. Pearson[5], V. Moulton[1] and T. Mock[3]*

**Marine phytoplankton are responsible for ~50% of the $CO_2$ that is fixed annually worldwide, and contribute massively to other biogeochemical cycles in the oceans[1]. Their contribution depends significantly on the interplay between dynamic environmental conditions and the metabolic responses that underpin resource allocation and hence biogeochemical cycling in the oceans. However, these complex environment–biome interactions have not been studied on a larger scale. Here we use a set of integrative approaches that combine metatranscriptomes, biochemical data, cellular physiology and emergent phytoplankton growth strategies in a global ecosystems model, to show that temperature significantly affects eukaryotic phytoplankton metabolism with consequences for biogeochemical cycling under global warming. In particular, the rate of protein synthesis strongly increases under high temperatures even though the numbers of ribosomes and their associated rRNAs decreases. Thus, at higher temperatures, eukaryotic phytoplankton seem to require a lower density of ribosomes to produce the required amounts of cellular protein. The reduction of phosphate-rich ribosomes[2] in warmer oceans will tend to produce higher organismal nitrogen (N) to phosphate (P) ratios, in turn increasing demand for N with consequences for the marine carbon cycle due to shifts towards N-limitation. Our integrative approach suggests that temperature plays a previously unrecognized, critical role in resource allocation and marine phytoplankton stoichiometry, with implications for the biogeochemical cycles that they drive.**

The global surface ocean is divided into distinct latitudinal temperature zones, ranging from ~30 °C in the tropics to the freezing temperature of seawater (~ − 1.8 °C) at the ocean polar sea/ice interface (inside sea ice, the temperature may be well below −1.8 °C). Phytoplankton, which fuel the entire ocean food web, inhabit all these temperature zones and their growth and diversity depend on their temperature optima for growth[3], and on temperature driven physical constraints such as stratification and mixing for the supply of nutrients[4]. Thus, temperature determines life in the surface ocean in manifold ways. Global climate change will redirect the fine-tuned balance between temperature and the biological evolution of phytoplankton in the global upper ocean. Recent data, although debated, indicate that increasing sea surface temperatures over the past century have caused a decline of about 1% of the global phytoplankton standing stock per year[5]. Thus, anthropogenic global warming could be responsible for a significant decline in phytoplankton since the 1950s. The majority of the diminishing phytoplankton belongs to the group of larger eukaryotic phytoplankton, such as the diatoms. According to older estimates, diatoms contribute to 25% of global carbon fixation[1]. However, according to a model study[6], their contribution might have decreased in the context of global warming. Despite the significance of temperature for life in surface oceans, we have only a limited understanding of its impact on the growth strategies, metabolism, and composition of eukaryotic marine phytoplankton[7]. Our integrative approach to this problem combines insights from metatranscriptomes and biochemical data with a model representation of ecological and evolutionary processes. Different existing models capture phytoplankton ecophysiology[8], stoichiometry[9] and diversity[10,11]. Our new modelling approach brings all these elements together, uniquely capturing phytoplankton cellular resource allocation and adaptation within physiological constraints, in a global model. The model represents major sub-cellular components within individual phytoplankton cells. These in turn form diverse populations in each grid point of an ocean general circulation model, which subjects the individuals to environmental selection, producing emergent growth strategies[12]. Here we use our overall integrative approach to show that temperature has a significant impact on cellular resource allocation and predict an altered N:P stoichiometry.

We sequenced marine eukaryotic phytoplankton metatranscriptomes from polar, temperate and tropical temperature zones of the ocean, including samples from both poles (Fig. 1a and Supplementary Fig. S1 and Table S1). We obtained about 1.5 million high quality cDNA sequences with an average length of ~242 bp (Supplementary Table S2). Although the size of this metatranscriptome dataset is limiting, representative biogeochemical provinces from low-temperature nutrient-rich coastal to high-temperature open-ocean high-nutrient low-chlorophyll waters have been sampled. Rarefraction curves based on the domain oriented Pfam database[13] demonstrated a levelling off with increased sequences for all metatranscriptomes (Supplementary Fig. S2), indicating a near saturated identification of known protein families. The majority of sequences were ecosystem-specific, based on CD-HIT (ref. 14) clustering using 60% similarity and 50% overlap of translated amino acid sequences (Fig. 1b). A significant proportion of transcripts from all samples closely resembled sequences

[1]School of Computing Sciences, University of East Anglia, Norwich Research Park, Norwich NR4 7TJ, UK, [2]College of Life and Environmental Sciences, University of Exeter, EX4 4SB, UK, [3]School of Environmental Sciences, University of East Anglia, Norwich Research Park, Norwich NR4 7TJ, UK, [4]Alfred-Wegener Institute for Polar and Marine Research, Bremerhaven, 27570, Germany, [5]Centre of Marine Sciences, University of the Algarve, Faro 8005-139, Portugal. *e-mail: t.mock@uea.ac.uk

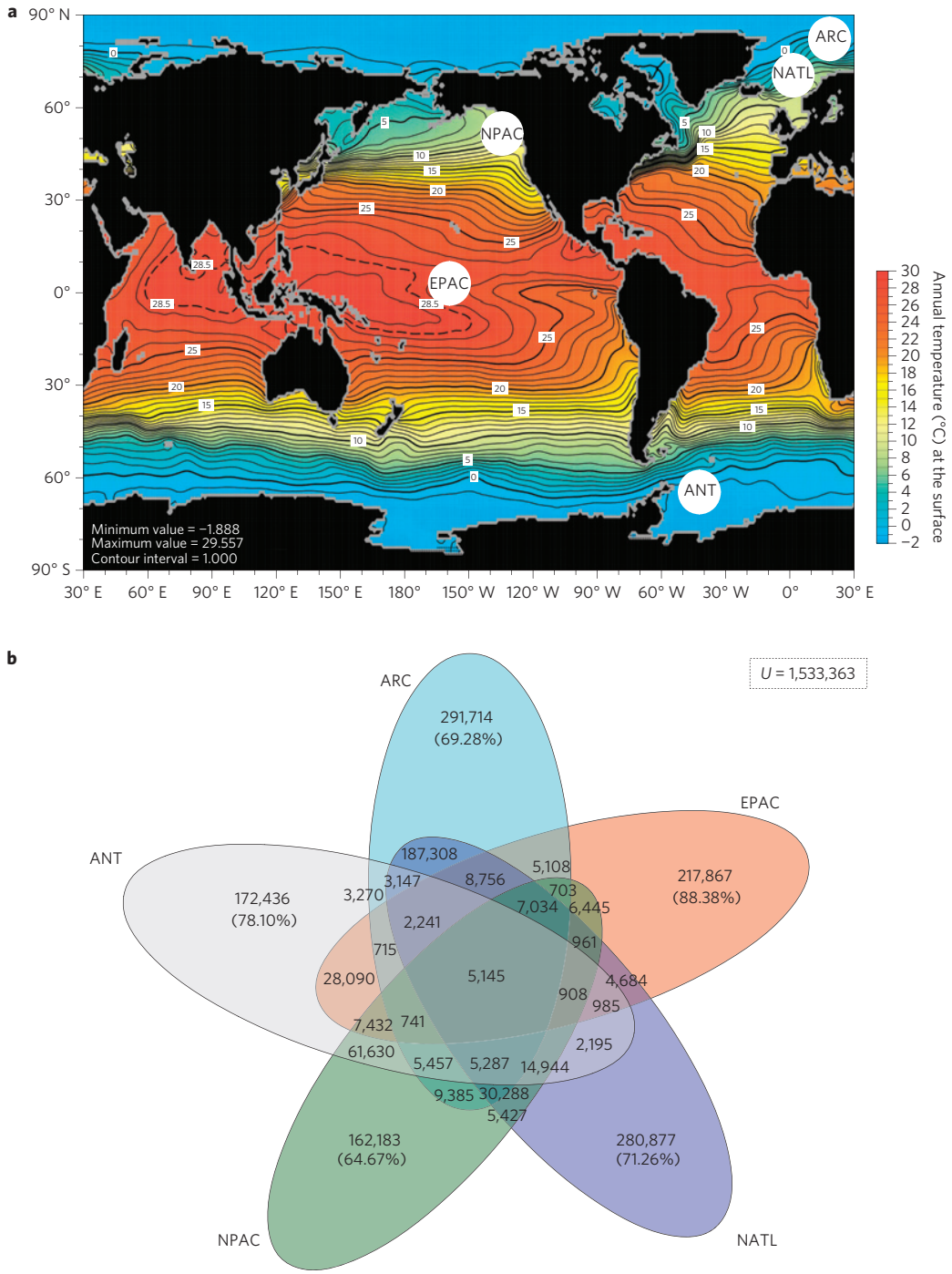


**Figure 1 | Sampling sites for eukaryotic phytoplankton metatranscriptomes and sequence distribution. a**, Sampling sites and surface ocean temperatures. Two stations each were sampled for EPAC and ANT. **b**, Sequence-distribution Venn diagram for pooled sequence clustering based on CD-HIT (longest open reading frames clustered using 60% similarity and 50% overlap of sequences). *U* is all sequences under consideration, numbers show sequences that fall into clusters from the environment(s) represented by that section of the Venn diagram. Percentages show the proportion of sequences that are specific to a particular environment. Part **a** is reproduced with permission from the World Ocean Atlas 2009 (http://data.nodc.noaa.gov/woa/WOA09F/temperature/JPEG/t_0_0_1.jpg), © National Oceanic and Atmospheric Administration/Department of Commerce.

(Genomic, EST or other) from known eukaryotic phytoplankton phyla (Supplementary Table S3 and Fig. S3). Samples from all five ecosystems differ significantly in terms of their taxonomic composition at the phylum level (PhymmBL (ref. 15) confidence score $\geq 0.9$; Fig. 2a) and did not show a correlation with temperature. Both polar samples and samples from the North Pacific Ocean (NPAC) were dominated by sequences from Bacillariophyta, whereas sequences from dinoflagellates dominated samples from the Equatorial Pacific Ocean (EPAC) and Ciliophora dominated samples from the North Atlantic Ocean (NATL; Fig. 2a). However, a functional annotation of sequences (GO term: biological processes[16]) revealed a significant clustering of metabolism according to the annual average surface ocean temperature, regardless of the taxonomic composition of the communities and significant differences in nutrient concentrations (for example, open ocean versus coastal; Fig. 2b), time of sampling and water depth. A canonical correspondence analysis (CCA)

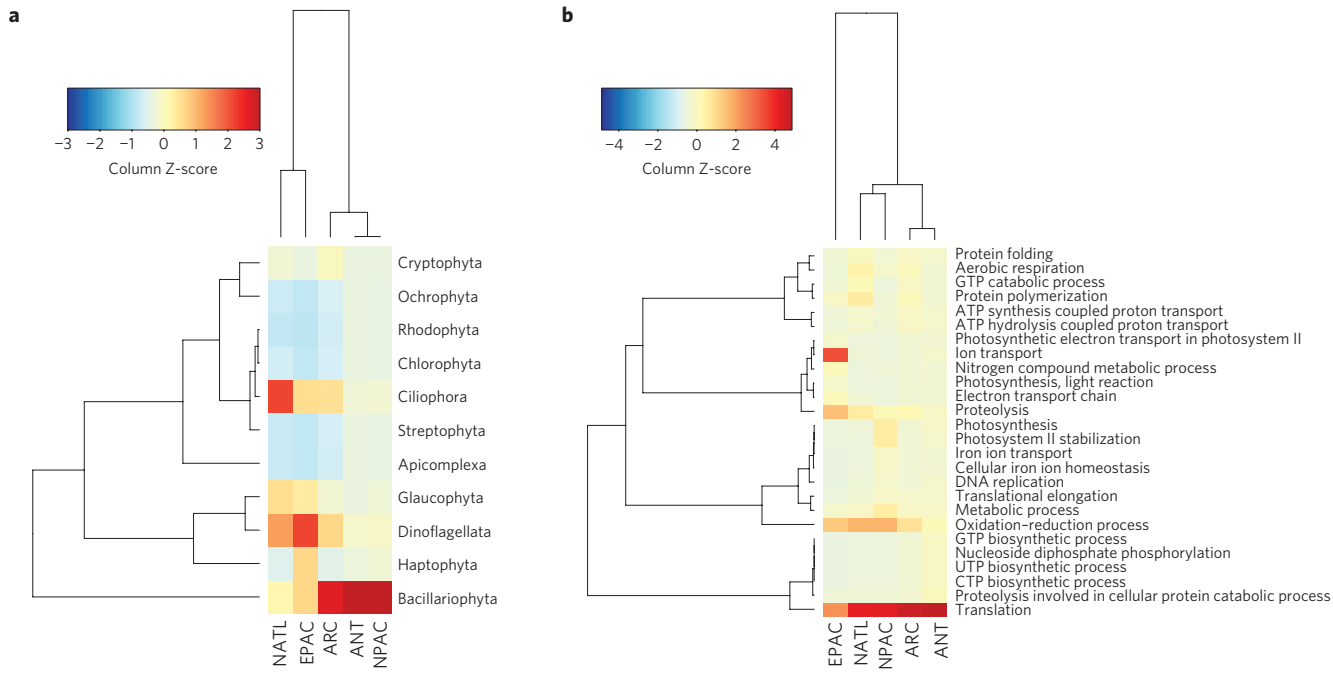


**Figure 2 | Heatmaps for algal groups and biological processes. a**,**b**, Heatmaps for PhymmBL-classified algal groups (confidence score of ≥0.9) (**a**) and biological process GO terms for all sequences (using an abundance cut off ≥0.5% of total GO terms in at least one environment) (**b**). Complete linkage clustering was performed based on a correlation matrix (1 − Pearson correlation coefficient) of relative abundances. Heatmaps scaled and centred by column (Z-score).

between protein family abundance, properties of the sequences (GC content), latitude, longitude and environmental conditions (light, temperature, nitrate, silicate, phosphate, salinity; Supplementary Table S4), deduced from ocean samples and annual averages for the corresponding sample locations, revealed that temperature accounts for 28.32% of metabolic variability, which is similar to both nitrate and phosphate (31.71% and 34.87%, respectively; Fig. 3a and Supplementary Fig. S4) and light (30.17%). This result indicates that temperature affects phytoplankton metabolism nearly as significantly as nutrients and light. Translation of proteins, as a core metabolic process, was identified to be strongly affected by temperature (Fig. 3a and Supplementary Fig. S5). A multicorrelation analysis based on the normalized abundance of sequences involved in translation (GO term: 0006412) revealed that temperature has the strongest correlation ($R = 0.9$) in comparison to all other tested environmental variables (Supplementary Fig. S6).

Biochemical studies on the eukaryotic ribosomal protein S14 in the psychrophilic Southern Ocean diatom *Fragilariopsis cylindrus* after acclimation to different temperature regimes (−2 to 10 °C) showed that this protein (Fig. 3b) is more abundant under low temperatures (−2 °C), corresponding to temperatures at the sea/ice interface. The regulation of transcripts encoding several other ribosomal proteins in *F. cylindrus* showed the same temperature dependence (Supplementary Fig. S7). A similar temperature dependence of the S14 ribosomal protein was observed in the globally distributed temperate diatom *Thalassiosira pseudonana* (Fig. 3b). However, the greatest difference in terms of protein abundance was observed between 11 and 20 °C in temperature regimes from 4 to 27 °C (Fig. 3b). Interestingly, the average annual surface temperature of 20 °C corresponds to tropical marine ecosystems (Fig. 1a).

It is evident from these data that temperature has an impact on the core metabolism in eukaryotic phytoplankton. Translation initiation at the ribosomes might be the rate-limiting step for protein synthesis under low temperatures and may therefore serve as a molecular thermometer in future studies to assess the impact of temperature on core metabolism in eukaryotic phytoplankton. Despite evidence that low temperatures increase the abundance of ribosomes, the rate of protein synthesis per cell seems to decrease at lower temperatures, on the basis of translation efficiency experiments with *T. pseudonana* at 11 and 20 °C (Fig. 3c). Translation efficiency was measured with temperature acclimated transgenic *T. pseudonana* cell lines that express green fluorescent protein (GFP) when nitrate is present in the growth medium. Translation efficiency was expressed as a rate constant ($m_{GFP}$), reflecting the increase of GFP fluorescence over time (Fig. 3c) after the addition of nitrate to N-starved cultures. Although an almost 3-fold difference in translation efficiency was observed between the two temperatures, the difference in response to nitrate addition (lag time) was below 1.5-fold. This suggests that increasing cellular concentrations of ribosomal proteins partially compensate for the reduced translation efficiency under low temperatures, which has implications for how fast cells are able to progress through the cell cycle and, hence, their ability to build up biomass[17–19].

Our NPAC samples were taken from a subsurface bloom (8 m) of nutrient-replete 12 °C water (Supplementary Fig. S8) dominated by *Thalassiosira*, *Chaetoceros* and *Coscinodiscus* species (Supplementary Table S5). When we selected only Bacillariophyta sequences (PhymmBL confidence score ≥0.9) from the NPAC metatranscriptome data set and aligned them to *T. pseudonana* genes significantly up-regulated (fold change >2, p-value <0.05; Supplementary Table S6) under limiting N, Si, Fe, $CO_2$ and low temperature[20], we found that 90% of them were homologs to genes up-regulated at low temperature (Supplementary Fig. S9). Among these, ribosomal transcripts dominated (Supplementary Table S7), followed by transcripts encoding heat shock proteins, DEAD-box ribonucleic acid (RNA) helicases and fatty acid desaturases, providing further evidence that metabolism in the diatom NPAC community represents a low-temperature-adapted transcriptome, with ribosome production as the most dominant core metabolism.

A higher production of ribosomes requires increased concentrations of rRNAs, because rRNAs and ribosomal proteins are produced in equimolar amounts[21]. rRNAs in eukaryotes in

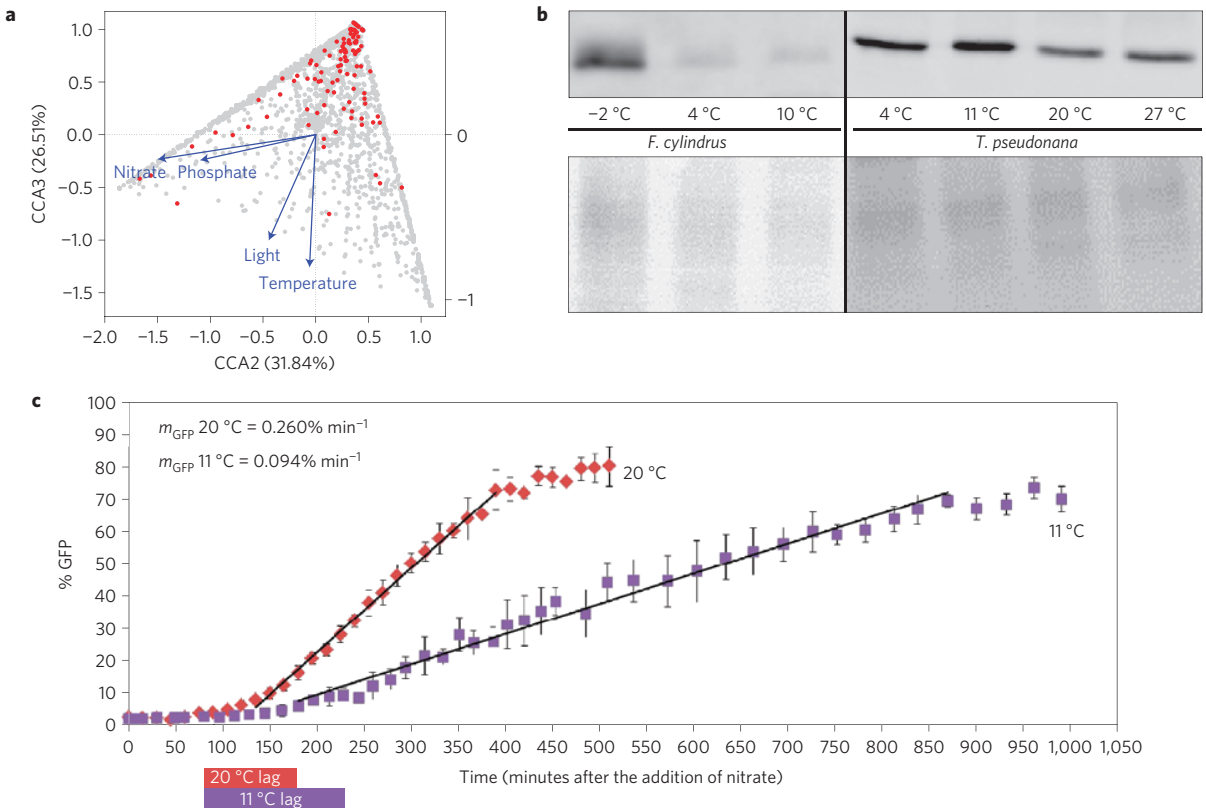


**Figure 3 | The impact of temperature on translation. a**, Canonical correspondence analysis between protein family (Pfam) abundance and environmental conditions deduced from ocean samples in this study, red dots represent ribosomal transcripts. Percentages on the axes show the proportion of variability accounted for by that dimension. **b**, Western blots using a commercial antipeptide against the eukaryotic ribosomal protein S14. Cultures of *F. cylindrus* and *T. pseudonana* were cultivated at different temperatures under nutrient replete conditions. **c**, Measurements of translation induction (lag time) and efficiency (slope) at different temperatures in *T. pseudonana* based on an inducible promoter (NR) and measurements of % eGFP increase over time ($N = 3$; error bars denote standard deviation; $m_{GFP}$ = constant for % eGFP increase per minute). The two bars below the plot indicate the length of the lag phase in minutes. The lag phase is the time required for the GFP signal to significantly ($p$-value $\leq 0.01$) rise above the background noise.

general contribute about 80% of total RNAs (ref. 22) in a cell because of their importance for translation; hence, the majority of substrates from purine and pyrimidine metabolism are used for rRNA synthesis[21,22]. The proportion of sequences from our metatranscriptomes encoding enzymes involved in purine and pyrimidine metabolism based on Kyoto Encyclopedia of Genes and Genomes (KEGG; ref. 23) assignments were negatively affected ($R = 0.96$) by increasing temperatures (Supplementary Fig. S10). The highest relative proportion of these sequences was identified in both polar metatranscriptomes, indicating a greater rate of RNA (mainly rRNA) synthesis, which is consistent with an increased content of ribosomes in the cells. Indeed, total RNA per cell in the polar diatom *F. cylindrus* markedly increased (about 2-fold) over a temperature gradient from +10 to −2 °C (Supplementary Fig. S11), similar to the increase of the eukaryotic ribosomal protein S14 at −2 °C (Fig. 3b). These data, together with the metatranscriptome data, provide unambiguous evidence that temperature in the ocean significantly affects phytoplankton core metabolism (synthesis of proteins and RNA), with consequences for resource allocation.

To put these results in a global context and test the hypothesis that they reflect adaptive physiological responses of cellular allocation to the environment, we developed a mechanistic phytoplankton cell model (Fig. 4a). This model resolves cell size and sub-cellular resource allocation to biosynthetic and photosynthetic pathways, which determine ecological traits and cellular stoichiometry. Environmental selection in a trait-based global marine ecosystems model then links emergent growth and cellular resource allocation strategies to large-scale patterns in light, nutrients and temperature in the marine environment. Optimal allocation to the biosynthesis component (Fig. 4b), including ribosomal proteins and rRNA, is related to the growth rate, and hence to a combination of light availability, nutrient availability and temperature. Nutrient availability demarcates resource-limited oligotrophic gyres with low allocation to biosynthesis from upwelling and bloom-forming regions with high allocation to biosynthesis. The assumed temperature dependence of biosynthesis superimposes a latitudinal gradient on this.

These global predictions for cellular resource allocation (Fig. 4b) are broadly consistent with the patterns in metatranscriptome data. For instance, a pair-wise gene ontology enrichment analysis between the two most contrasting ecosystems in terms of temperature (ANT (Southern Ocean) versus EPAC, Supplementary Fig. S12) revealed that processes involved in translation (identified with model rRNA and component $E$, Supplementary Fig. 3) were significantly enriched in the ANT metatranscriptome, whereas membrane associated processes involved in ion transport (identified with $S$, Supplementary Fig. S13), photosynthesis and respiration were significantly enriched in the EPAC metatranscriptome. A model for optimal cellular allocation under nutrient-replete exponential growth (appropriate for diatom ecological strategies from boom to bust) demonstrates the temperature-dependent reciprocal resource investment into photosynthesis versus biosynthesis (with a large contribution from ribosomal proteins and rRNA; Supplementary Fig. S14). Under low temperatures, cells invest more in biosynthesis, whereas under high temperatures more resources are invested in photosynthesis. Investment in biosynthesis significantly

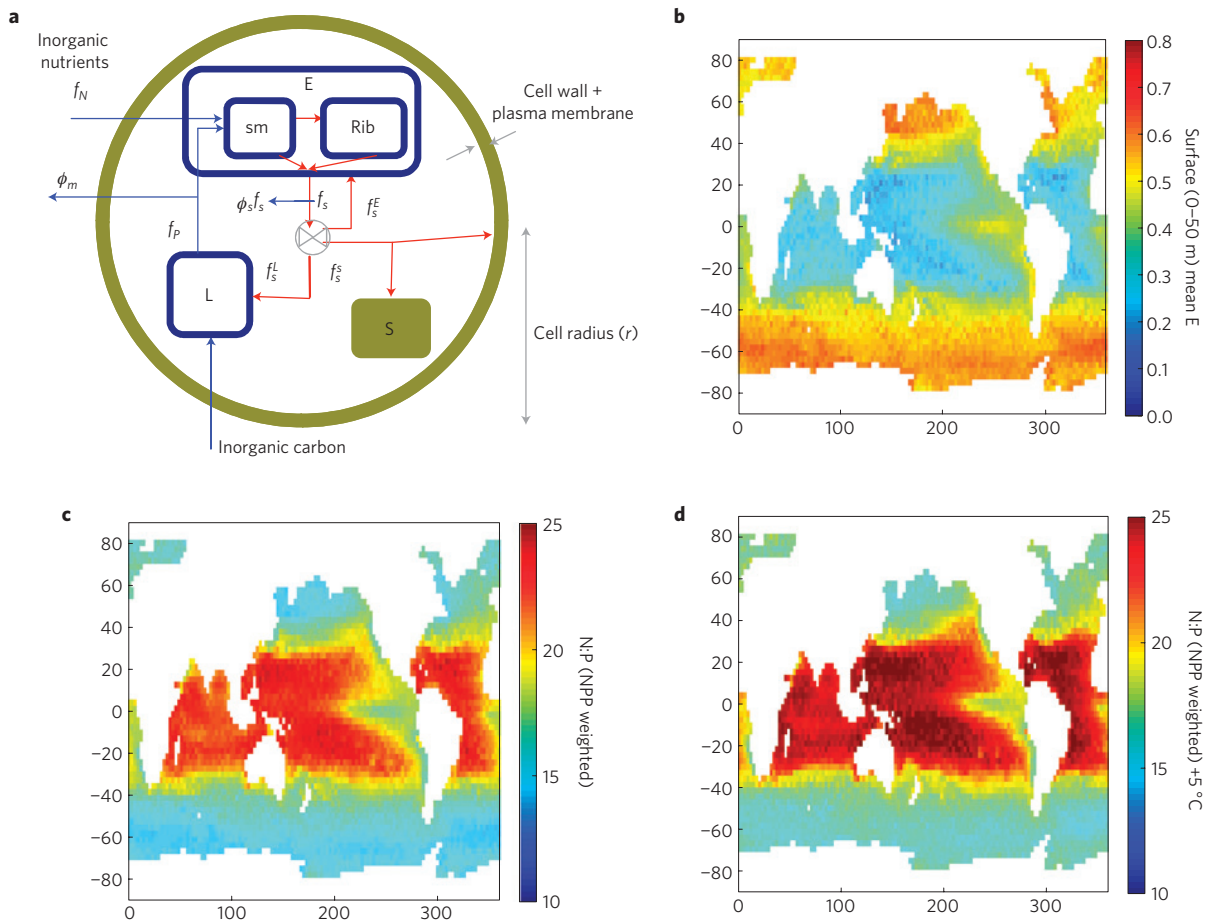


**Figure 4 | Phytoplankton cell model and N:P ratios. a**, Cell model containing light-harvesting apparatus (L) (Chlorophyll, accessory pigments), biosynthesis (E) (small molecule biosynthesis (sm) and ribosomes (rib)) and cell structure (S) (including nutrient acquisition and assimilation). Carbon, nutrients and energy (blue arrows) are synthesized to new biomass (red arrows) which is allocated (crossed circle) to cellular compartments. **b**, Relative cellular allocation to biosynthesis in a global ecosystem model. **c**, Modelled N:P ratios based on cell and ecosystems model in **a**,**b**. **d**, Sensitivity study showing N:P for a +5 °C perturbation to the 'physiological' temperature in an unchanged climate.

increases under higher light intensities, but the sensitivity to temperature remains the same.

The global model demonstrates that allocation to phosphate-rich rRNAs significantly alters the N:P stoichiometry of marine phytoplankton according to latitudinal changes in temperature and nutrient availability (Fig. 4c). The lowest N:P is predicted in colder regions and those with upwelling nutrients. The highest N:P is predicted in warm stratified sub-tropical gyres. Indeed, the most recent analysis provides evidence for the temperature dependence of marine plankton and organic matter N:P ratios on a global scale, with temperature explaining 33% of the variation ($R^2$) in N:P ratios[24]. Plant leaf N:P ratios have also been shown to be strongly correlated with the mean annual temperature of terrestrial ecosystems[25]. Thus, temperature-dependent changes of N:P ratios in autotrophic organisms seem to be universal[24,25]. However, as growth rates are generally much lower in terrestrial plants, the physiological basis of these biogeographic patterns may differ, with lower rRNA contributions to bulk P and an increased importance of other factors such as protein turnover in determining rRNA content[2]. The mechanisms and relative importance of multiple temperature-correlated environmental controls (including nutrient supply) also differ between terrestrial and marine environments.

The integrated response of the marine ecosystem to climate change will include both the 'direct' effects of temperature on physiology and the 'indirect' effects due to ocean stratification changes[6,26]. To isolate the 'direct' effect on N:P stoichiometry, we performed an idealized sensitivity study by perturbing the temperature seen by the cell physiology by +5 °C in an unchanged climate. Figure 4d shows that 'direct' temperature effects on physiology lead to an overall increase in N:P at higher temperature. There are two effects involved. At low latitudes ($\sim < 30°$), growth is resource limited and a change in 'physiological temperature' has a large relative effect on allocation to biosynthesis and rRNA; however as the absolute allocation to biosynthesis is small, this has only a small overall effect on N:P. At high latitudes, growth is exponential. Increased temperature has a large direct effect on growth rate[27], but a smaller effect on the relative allocation to rRNA, as rRNA makes a higher absolute contribution to cellular allocation (Supplementary Fig. S14).

Our integrated ecosystems approach therefore demonstrates that the 'direct' metabolic response to environmental temperature change[28–30], especially in polar and temperate marine ecosystems, will have a significant impact on the ecological and biogeochemical cycling of N and P (ref. 9). Specifically, global warming and associated ocean stratification may be expected to increase the N:P ratios of eukaryotic phytoplankton. This will tend to increase N limitation in the ocean, but may also increase export fluxes of carbon, given that C:N is relatively conserved[24]. These data add to concerns about the effect of global warming on marine ecosystem functioning.

## Methods

**Metatranscriptomics.** Natural phytoplankton communities were sampled from polar (Southern Ocean, Arctic Ocean (ARC)), temperate (North Atlantic,

Northwest Pacific) and tropical (Central Equatorial Pacific) surface marine ecosystems. The samples were purified for mRNA, reverse transcribed into double-stranded cDNA and sequenced using a combination of 454 GS-FLX and titanium pyrosequencing. Quality-filtered sequences were taxonomically classified using PhymmBL (extended with eukaryotic genome and EST-interpolated Markov models). Transcript functions were assigned using sequence homology to Pfam protein domains, gene ontology terms and KEGG orthologies. Canonical correspondence analysis was performed based on relative Pfam abundances for all sequences. Details are described in Supplementary Information S1,S2,S3 and S5.

**Molecular physiology and biochemistry.** Temperature experiments were conducted with the mesophilic diatom *T. pseudonana* and the psychrophilic diatom *F. cylindrus*. Quantitative PCR and Western blots were used to investigate the temperature-dependent expression of ribosomal genes and their proteins. A transgenic *T. pseudonana* cell line expressing eGFP regulated by an inducible nitrate reductase promoter was used to measure the translation efficiency ($m_{GFP}$) at 11 and 20 °C. *F. cylindrus* was used to measure temperature-dependent changes in the concentration of cellular RNA. Details are described in Supplementary Information S4.

**Modelling.** The phytoplankton cell model represents allocation to three components: $L$ represents cellular resource allocation (fraction of cell nitrogen) to the photosynthetic light harvesting apparatus (including chlorophyll and accessory pigments); $E$ represents allocation to the biosynthetic apparatus (including aggregated enzyme systems and ribosomes involved in small and large molecule biosynthesis); and $S$ represents a size-dependent allocation to cell structure, including cell surface associated components involved in nutrient acquisition and assimilation, and all 'other' components not directly involved in either photosynthesis or biosynthesis. Growth rate is then given by the most limiting of the light-harvesting mass-specific rate, $f_p = k_p I_z L$ (where $I_z$ is incident light intensity and $k_p$ is an empirically determined rate constant), the temperature-dependent biosynthesis rate, $k_s Q_{10}^{(T-T_0)/10} E$ (where temperature dependence is represented by the factor $Q_{10}$, and $k_s$ is an empirically determined rate constant), and the mass-specific nutrient uptake (assumed diffusion limited and hence related to cell radius $r$ by $f_N \propto 1/r^2$). New biomass (at rate $f_s$, accounting for cost of biosynthesis $\phi_s$ and maintenance $\phi_m$) is allocated to cellular pools at rates $f_S^L$, $f_S^E$ and $f_S^S$. Resource allocation strategies in the global individual-based marine ecosystem model are set by traits, which are acted on by environmental selection. In the simplified optimality model, resource allocation to $L$ and $E$ (including ribosomes) under steady-state environmental conditions (light, temperature, unlimited nutrients) is set by maximization of the mass-specific growth rate. The minimum cellular rRNA to protein ratio by dry mass $r^{mass}_{cellrRNA:prot}$ required for growth is given in terms of the growth rate $\mu$ and the per-ribosome synthesis rate $\phi_a\sigma_a$ by $r^{mass}_{cellrRNA:prot} = 5.9(\mu/1\,h^{-1})(\phi_a\sigma_a/1\,\text{aa rib}^{-1}\text{s}^{-1})$. Details are described in Supplementary Information S6.

Received 27 March 2013; accepted 29 July 2013; published online 8 September 2013

## References


1. Field, C. B., Behrenfeld, M. J., Randerson, J. T. & Falkowski, P. G. Primary production of the biosphere: Integrating terrestrial and oceanic components. *Science* **281,** 237–240 (1998).
2. Elser, J. J., Fagan, W. F., Kerkhoff, A. J., Swenson, N. G. & Enquist, B. J. Biological stoichiometry of plant production: Metabolism, scaling and ecological response to global change. *New Phytol.* **186,** 593–608 (2010).
3. Thomas, M. K., Kremer, C. T., Klausmeier, C. A. & Litchman, E. A global pattern of thermal adaptation in marine phytoplankton. *Science* **338,** 1085–1088 (2012).
4. Falkowski, P. G., Barber, R. T. & Smetacek, V. Biogeochemical controls and feedbacks on ocean primary production. *Science* **281,** 200–206 (1998).
5. Boyce, D. G., Lewis, R. M. & Worm, B. Global phytoplankton decline over the past century. *Nature* **466,** 591–596 (2010).
6. Bopp, L., Aumont, O., Cadule, P., Alvain, S. & Gehlen, M. Response of diatoms distribution to global warming and potential implications: A global model study. *Geophys. Res. Lett.* **32,** L19606 (2005).
7. Schlesinger, D. A. & Shuter, B. J. Patterns of growth and cell composition of freshwater algae in light-limited continuous cultures. *J. Phycol.* **17,** 250–256 (1981).
8. Shuter, B. A model of physiological adaptation in unicellular algae. *J. Theoret. Biol.* **78,** 519–552 (1979).
9. Weber, T. S. & Deutsch, C. Oceanic nitrogen reservoir regulated by plankton diversity and ocean circulation. *Nature* **489,** 419–422 (2012).
10. Follows, M. J., Dutkiewicz, S., Grant, S. & Chisholm, S. W. Emergent biogeography of microbial communities in a model ocean. *Science* **315,** 1843–1846 (2007).
11. Bruggeman, J. & Kooijman, S. A. L. M. A biodiversity-inspired approach to aquatic ecosystem modeling. *Limnol. Oceanogr.* **52,** 1533–1544 (2007).
12. Clark, J. R., Lenton, T. M., Williams, H. T. P. & Daines, S. J. Environmental selection and resource allocation determine spatial patterns in picophytoplankton cell size. *Limnol. Oceanogr.* **58,** 1008–1022 (2013).
13. Finn, R. D. *et al.* The Pfam protein families database. *Nucleic Acids Res.* **38** (suppl. 1), D211–D222 (2010).
14. Li, W. & Godzik, A. Cd-hit: A fast program for clustering and comparing large sets of protein or nucleotide sequences. *Bioinformatics* **22,** 1658–1659 (2006).
15. Brady, A. & Salzberg, S. L. Phymm and PhymmBL: Metagenomic phylogenetic classification with interpolated Markov models. *Nature Methods* **6,** 673–676 (2009).
16. Ashburner, M. *et al.* Gene Ontology: Tool for the unification of biology. *Nature Genet.* **25,** 25–29 (2000).
17. Nomura, M., Grouse, R. & Baughman, G. Regulation of the synthesis of ribosomes and ribosomal components. *Annu. Rev. Biochem.* **53,** 75–117 (1984).
18. Fraser, K. P. P., Clarke, A. & Peck, L. S. Low-temperature protein metabolism: Seasonal changes in protein synthesis and RNA dynamics in the Antarctic limpet *Nacella concinna* Strebel 1908. *J. Exp. Biol.* **205,** 3077–3086 (2002).
19. Kim, K-Y. *et al.* Molecular cloning of low-temperature-inducible ribosomal proteins from soybean. *J. Exp. Bot.* **55,** 1153–1155 (2004).
20. Mock, T. *et al.* Whole-genome expression profiling of the marine diatom *Thalassiosira pseudonana* identifies genes involved in silicon bioprocesses. *Proc. Natl Acad. Sci. USA* **105,** 1579–1584 (2008).
21. Woolford, J. L. J. & Warner, J. R. in *The Molecular And Cellular Biology of Yeast Saccharomyces: Genome Dynamics, Protein Synthesis And Energetics* (eds Broach, J. R., Pringle, J. R. & Jones, E. W.) 587–625 (Cold Spring Harbor Laboratory Press, 1991).
22. Warner, J. R. The economics of ribosome biosynthesis in yeast. *TIBS* **24,** 437–440 (1999).
23. Kanehisa, M. & Goto, S. KEGG: Kyoto Encyclopedia of Genes and Genomes. *Nucleic Acids Res.* **28,** 27–30 (2000).
24. Martiny, A. C., Pham, C. T. A., Primeau, F. W., Vrugt, J. A., Moore, J. K., Levin, S. A. & Lomas, M. W. Strong latitudinal patterns in the elemental ratios of marine plankton and organic matter. *Nature Geosci.* **6,** 279–283 (2013).
25. Reich, P. B. & Oleksyn, J. Global patterns of plant leaf N and P in relation to temperature and latitude. *Proc. Natl Acad. Sci. USA* **101,** 11001–11006 (2004).
26. Doney, S. C. Oceanography: Plankton in a warmer world. *Nature* **444,** 695–696 (2006).
27. Eppley, R. Temperature and phytoplankton growth in the sea. *Fish. Bull.* **70,** 1063–1085 (1972).
28. Brown, J. H., Gillooly, J. F., Allen, A. P., Savage, V. M. & West, G. B. The Robert H. MacArthur Award Lecture-toward a metabolic theory of ecology. *Ecology* **85,** 1771–1789 (2004).
29. Allen, A. P. & Gillooly, J. F. Towards an integration of ecological stoichiometry and the metabolic theory of ecology to better understand nutrient cycling. *Ecol. Lett.* **12,** 369–384 (2009).
30. Regaudie-de-Gioux, A. & Duarte, C. M. Temperature dependence of planktonic metabolism in the ocean. *Glob. Biogeochem. Cycles* **26,** 1–10 (2012).


## Acknowledgements

Sequencing of ANT, EPAC and NPAC was funded by a Natural Environment Research Council (NERC) grant (MGF (NBAF) grant 197) and a 454 Life Sciences grant (Roche, 10Gb grant) awarded to T.M. and K.V. K.V. acknowledges the DFG for funding. Sequencing of ARC and NATL was funded by the EU FP7 project 'Arctic Tipping Points' awarded to G.A.P. We thank The Genome Analysis Centre (TGAC) in Norwich and Melanie Febrer for facilitating the work with 454 Life Sciences (Roche) in the US and UK. S.J.D., J.R.C. and T.M.L. acknowledge the Leverhulme Trust (F/00 204/AP) for funding. The PhD studentship of A.T. was funded by the Earth and Life Systems Alliance (ELSA) in Norwich. A.K. and T.M. acknowledge the Leverhulme Trust (F/00204/AU) for funding. Part of the bioinformatic analysis was performed on the High Performance Computing Cluster supported by the Research and Specialist Computing Support service at the University of East Anglia. We thank S. Moxon for his patient support, discussions and suggestions. We thank W. Guo and A. Marchetti for providing us with samples from EPAC and M. Parker, E. V. Armbrust, and the 'Sorcerer II' crew (JCVI) for assistance with sampling of NPAC. G.A.P. acknowledges A. Ramos, E. Serrão and the crew of R/V Jan Mayen, University Tromso, Norway for assistance with sampling of ARC and NATL.

## Author contributions

Metatranscriptome sample preparation: T.M., G.A.P., K.V. and C.U.; Bioinformatics: A.T. and V.M.; Western blots: A.K.; Quantitative PCR: J.S.; Growth experiments: A.K., J.S. and T.M.; Modelling: S.J.D., J.R.C., T.M.L.; T.M. designed the study and wrote the manuscript with help from S.J.D. and T.M.L. All authors discussed the results and commented on the manuscript.

## Additional information

Supplementary information is available in the online version of the paper. Reprints and permissions information is available online at www.nature.com/reprints. Correspondence and requests for materials should be addressed to T.M.

## Competing financial interests

The authors declare no competing financial interests.